Transmission and Backscattering of 4.0- to 12.0-MeV Electrons*

P. J. EBERT, A. F. LAUZON, AND E. M. LENT
Lawrence Radiation Laboratory, University of California, Livermore, California 94550
(Received 31 January 1969)

Transmission and backscattering coefficients were measured for 4.0- to 12.0-MeV monoenergetic electrons normally incident on solid targets of C, Al, Cu, Ag, Ta, and U. Transmitted and backscattered electrons were collected by biased Faraday cups, each subtending ~90% of 2π sr. Number transmission coefficients at 10 MeV agree with Berger and Seltzer's Monte Carlo results, and saturation backscattering coefficients generally agree with Tabata's results to within ±10%. Empirical formulas for determining the extrapolated range and both the transmission and backscattering coefficients as a function of Z, energy, and thickness have been developed.

I. INTRODUCTION

ENERGETIC electrons incident on a solid target are transmitted through, absorbed in, and backscattered from the target. Also associated with these phenomena is the emission of both low-energy (<100 eV) and high-energy (δ rays) secondary electrons. Transmission coefficients (electrons transmitted through a semi-infinite slab of material per incident electron) for electrons having energy greater than 1 MeV are relatively scarce. Most experiments have been performed below 1 MeV on Al targets. Data prior to 1952 have been reviewed by Katz and Penfold.[1] Seliger[2] and Agu *et al.*[3] have measured transmission coefficients of less than 1-MeV electrons in a number of elements. Monte Carlo calculations have provided transmission coefficients for Al as well as other elements.[4–7] Birkhoff[8] and recently Zerby and Keller[9] have reviewed both the theoretical and experimental aspects of high-energy electron transport. Very little data on high-energy electron transmission were included in these reviews. Clearly, such data would provide useful checks on both the Monte Carlo results and experiments in which absolute differential energy spectra and angular distributions are measured.[10]

Backscattering coefficients have been reported by Wright and Trump,[11] Cohen and Koral,[12] Harder and Ferbert,[13] and more recently by Dressel[14] and by Tabata.[15] The backscattering coefficients reported by Dressel are roughly twice as large as those reported by Tabata, whose results are consistent with those of other workers.[11–13]

The following is a report of an experiment in which transmission coefficients and backscattering coefficients of 4.0- to 12.0-MeV electrons were measured for the elements C, Al, Cu, Ag, Ta, and U. A preliminary account of this work has been given previously.[16]

II. EXPERIMENT

A. General

A beam of monoenergetic electrons of current I_0 incident on a planar target is backscattered, absorbed, and transmitted. During time τ, a charge $Q_0=I_0\tau$ is incident. The transmission coefficient T is given by

$$T=Q_T/Q_0=Q_T/(Q_B+Q_A+Q_T), \quad (1)$$

where Q_T is the charge transmitted through the target, Q_A is the charge absorbed in the target, and Q_B is the charge backscattered from the target. The backscatter coefficient B is given by

$$B=Q_B/Q_0=Q_B/(Q_B+Q_A+Q_T) \quad (2)$$

and the absorption coefficient A is given by

$$A=Q_A/Q_0=Q_A/(Q_B+Q_A+Q_T). \quad (3)$$

Each of the above was measured as a function of electron energy, target thickness, and atomic number.

B. Electron Beam

The electron beam from the EG & G-AEC linac was deflected 90° into the experimental chamber by an analyzing magnet. Before energy analysis, the beam was collimated to a 0.3-cm diam. The beam energy spread, governed by the width of the Δr slit in the magnetic analyzer, was ±1%.[17] The analyzed beam was directed through two 0.3-cm-diam Cu collimators

* Work performed under the auspices of the U. S. Atomic Energy Commission.

[1] L. Katz and A. S. Penfold, Rev. Mod. Phys. **24**, 28 (1952).
[2] H. H. Seliger, Phys. Rev. **100**, 1029 (1955).
[3] B. N. C. Agu, T. Burdett, and E. Matsukawa, Proc. Phys. Soc. (London) **71**, 201 (1958); **72**, 727 (1958).
[4] J. E. Leiss, S. Penner, and C. W. Robinson, Phys. Rev. **107**, 1544 (1957).
[5] J. F. Perkins, Phys. Rev. **126**, 1781 (1962).
[6] M. J. Berger and S. Seltzer, National Aeronautics and Space Administration Report No. SP-71, 437, 1964 (unpublished).
[7] B. W. Mar, Trans. Am. Nucl. Soc. **7**, 322 (1964).
[8] R. D. Birkhoff, in *Handbuch der Physik*, edited by S. Flügge (Springer-Verlag, Berlin, 1958), Vol. 34.
[9] C. D. Zerby and F. L. Keller, Nucl. Sci. Eng. **27**, 190 (1967).
[10] J. A. Lonergan, C. P. Jupiter, and G. Merkel, Gulf General Atomic Report No. GA-8486, 1968 (unpublished).
[11] K. A. Wright and J. G. Trump, J. Appl. Phys. **33**, 687 (1962).
[12] A. J. Cohen and K. F. Koral, National Aeronautics and Space Administration Technical Note No. TND-2782, 1965 (unpublished).
[13] D. Harder and H. Ferbert, Phys. Letters **9**, 233 (1964).
[14] Ralph W. Dressel, Phys. Rev. **144**, 332 (1966).
[15] Tatsuo Tabata, Phys. Rev. **162**, 336 (1967).
[16] P. J. Ebert, A. F. Lauzon, E. M. Lent, and R. G. Der, Bull. Am. Phys. Soc. **11**, 890 (1966).
[17] C. Sandifer and W. D. George, EG & G Technical Report No. S-333-R, 1965 (unpublished).

1.0 cm thick and 40 cm apart. Copper was selected for the collimators as a compromise between a low-Z, low-density material, which produces a large low-energy secondary electron background, and a high-Z, high-density material, which produces a high bremsstrahlung background. The maximum beam diameter allowed by the collimators was 0.6 cm at the target.

The linac was adjusted for a beam pulse width of 2×10^{-6} sec and a repetition rate of 200 pulses/sec. Average beam current ranged between 10^{-8} and 10^{-6} A, depending on the electron energy.

C. Target Chamber

A target chamber of welded aluminum construction was fabricated in two sections and is shown in Fig. 1. In addition to the collimator assembly previously described, it contained x-ray shielding, an insulated target holder, two massive Faraday cups on either side of the target holder, and a carbon beam stopper between the collimators. Sufficient Pb shielding (5 cm) was placed in the drift tube behind each collimator to attenuate most of the x rays produced in the collimator. An equal thickness Pb shielding was placed close to the target chamber outside the drift tube. Each Faraday cup fit inside a 30.5-cm-i.d. cylinder. A 67-cm-diam section contained the target wheel. The chamber could be opened at the central large-diameter section for easy target access. The chamber section holding the backscattering cup was rigidly mounted to both the linac and a steel table. An oil diffusion pump with a liquid-nitrogen-cooled baffle and an ionization gauge were also connected to this section. All measurements were made with the pressure less than 1×10^{-4} Torr.

Electrons passing through the collimators and a 1.0-cm-diam hole in the bottom of the backscattering cup bombarded the target, which was held in a nonconducting wheel. The surface of the wheel was Al vapor-plated and grounded to minimize the effects of dielectric polarization on target charge. Separate wheels holding either 15 8-cm-diam targets or 22 2-cm-diam targets were used. A Geneva mechanism rotated the wheel to insure that each target was precisely aligned on the beam axis.

Transmitted and backscattered electrons were collected in massive Faraday cups. A 10-cm-i.d. carbon cup, 10 cm long and having a 1-cm-thick wall, was used to collect backscattered electrons. The outside of the cup was shielded by 5 cm of Pb. The cup entrance was collimated to 12 cm by a 0.15-cm-thick grounded Ta sheet. Transmitted electrons were collected in a 10-cm-i.d. carbon cup, 10 cm deep and having 1-cm-thick wall and a 3-cm-thick bottom. A matrix of holes 0.15-cm in diam and 0.8 cm deep was drilled over the entire bottom surface of the cup to further reduce backscatter. In addition to 5-cm-thick Pb shielding, a 10-cm-thick W shield was also placed in this assembly to minimize electron losses caused by bremsstrahlung produced in the target. The calculated transmission of 10-MeV x rays through the transmission cup is approximately 10^{-4}. Entrance collimation of the transmission cup was identical to that of the backscattering cup. The axial alignment of both cups was insured by sighting through the rear of the chamber down the collimator axis. When mounted to the accelerator, the experimental chamber was aligned by shining a laser beam down the axis of the drift tube through the collimators.

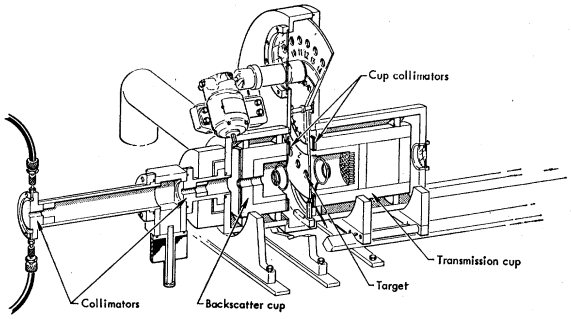

FIG. 1. Cutaway view of experimental chamber. Electrons enter collimators from left, pass through the backscattering cup, and are normally incident on target centered on the collimator axis by a Geneva mechanism.

In order to minimize very low-energy secondary electron current, bias rings were mounted in both Faraday cups. The rings, connected together electrically, were at half-angles of 45° and 80° with respect to the beam axis and cup entrance plane. At the beginning of the experiment, it was found that a negative bias in excess of −300 V caused no change in the current in either the Faraday cups or the target. The rings were biased at −500 V throughout the experiment.

D. Targets

Approximately 40 targets of each element investigated were fabricated. Thicknesses ranged from ~0.030 to ~6 g/cm². All targets were greater than 99% pure. Most targets were machined to the appropriate linear thickness and then weighed on an analytical balance. The diameters of the targets were measured either on a microscope comparator or with a micrometer caliper. The average thickness was determined by dividing the weight by the area of the target. The average target thickness determined in this way is accurate to within ±0.5%. Targets were either 2.0 or 8.0 cm diam. The large targets ranged in linear thickness from 0.6 to about 3.2 cm, fulfilling the requirement that target radius be greater than the sum of the beam radius and the electron maximum range in order to approximate a semi-infinite slab.

E. Current Integration

Current pulses from the target and Faraday cups were respectively fed via vacuum feedthroughs and ~40-m-long cable runs to three Elcor Model 310 B current integrators in the linac control room. When

possible, current ranges on all integrators were set so that the current read between 0.3 and 0.8 of full scale on the current indicator. With a zero thickness target in position, this condition could not be fulfilled on the target and backscattering cup integrators. Current integration began simultaneously in all three instruments when the master unit was activated. The integrator system was programmed to stop integrating when 50 charge counts were accumulated in any one of the integrators.

F. Experimental Error

1. Electron Energy

Electron energy was determined from measurement of magnetic field strength of the analyzing magnet and is accurate to $\pm 1\%$. The slit width was set at $\pm 1\%$ for all energies.

2. Current Integration

The current integrators were calibrated relative to each other to within one part in 10^3 using a Keithley Model 261 standard current source. The relative error in the total current integration as well as integration of the current in the Faraday cups and target was at most 0.17%. Since minor adjustments were made on the integrators during each day's calibration, a $\pm 0.2\%$ error is assigned for current integration.

3. Charge Collection

Error in charge collection consists of (a) electron background or unwanted electrons and (b) electron loss due to geometry. Background charge was determined in two ways:

(i) Current integrated with the carbon beam stopper intercepting the beam gave the background due to bremsstrahlung produced in the first collimator. Electrons bombarding this collimator presumably made this the most intense bremsstrahlung source since a considerable fraction ($\sim 90\%$) of the analyzed electron beam was stopped by the first collimator.

(ii) Charge due to secondary electron production in the second collimator was determined by integrating the current in the backscattering cup with a zero-thickness target in position. For this measurement, it was assumed that the transmission cup had 100% charge collection efficiency. This assumption is accurate, since backscattering from solid carbon at 4.0 MeV is $<1\%$.

Collection of unwanted background electrons was observed in the backscattering cup only, and was a function of electron energy. If it is assumed that the Faraday cups are 100% efficient electron absorbers, the backscattering coefficient from target of thickness $t=0$ is a measure of this background. The value of B at $t=0$ was nil at 4.0 MeV, and increased in roughly linear fashion to 2.6×10^{-3} at 12.0 MeV. Backscattering charge and the total charge were corrected for this background. The uncertainty in this correction is estimated to be $\pm 30\%$. The error due to secondary electron collection is mainly propagated to the backscattering coefficient of low-Z elements at the higher energies, and for the worst possible case of a carbon target at 12.0 MeV, an uncertainty $>100\%$ for a single measurement of B was possible. It should be noted that this large uncertainty in the backscattering has a very small effect ($<0.2\%$) on the transmission coefficients.

The solid angle subtended by the transmission cup was 90% of 2π sr. The particle loss is estimated to be 0.5%, assuming a $\cos\theta$ angular distribution of transmitted electrons. Losses in the backscattering cup were a function of target thickness, and ranged for the 8-cm-

TABLE I. Typical error in a single measurement on Al and U at 6.0 MeV.

		Transmission coefficient		Absorption coefficient		Backscattering coefficient	
		Al	U	Al	U	Al	U
Thick target ($T\approx 0.3$)							
Random error (%)	Current integration	0.2	0.2	0.2	0.2	0.2	0.2
	Particle loss	0.5	0.5	···	···	5	5
	Collimator background	0.1	0.1	0.1	0.1	3	0.3
	Target thickness	0.5	0.5	···	···	0.5	0.5
	Random rms error	0.8	0.8	0.2	0.2	6.1	5.1
Systematic error (%)	Electron energy	1	1	1	1	1	1
	Target purity	0.1	0.1	0.1	0.1	0.1	0.1
	Total systematic error	1.1	1.1	1.1	1.1	1.1	1.1
Total error (%)		1.9	1.9	1.3	1.3	7.2	6.2
Thin target ($T\approx 0.8$)							
Random error (%)	Current integration	0.2	0.2	0.2	0.2	0.2	0.2
	Particle loss	0.5	0.5	···	···	5	5
	Collimator background	0.1	0.1	0.1	0.1	10	1
	Target thickness	0.5	0.5	···	···	0.5	0.5
	Random rms error	0.8	0.8	0.2	0.2	11.2	5.1
Systematic error (%)	Electron energy	1	1	1	1	1	1
	Target purity	0.1	0.1	0.1	0.1	0.1	0.1
	Total systematic error	1.1	1.1	1.1	1.1	1.1	1.1
Total error (%)		1.9	1.9	1.3	1.3	12.3	6.2

TABLE II. Typical error in a single measurement on Al and U at 10.2 MeV.

		Transmission coefficient		Absorption coefficient		Backscattering coefficient	
		Al	U	Al	U	Al	U
Thick target ($T\approx0.3$)							
Random error (%)	Current integration	0.2	0.2	0.2	0.2	0.2	0.2
	Particle loss	0.5	0.5	...	...	5	5
	Collimator background	0.2	0.2	0.2	0.2	8	1.0
	Target thickness	0.5	0.5	...	...	0.5	0.5
	Random rms error	0.8	0.8	0.3	0.3	9.4	5.1
Systematic error (%)	Electron energy	1	1	1	1	1	1
	Target purity	0.1	0.1	0.1	0.1	0.1	0.1
	Total systematic error	1.1	1.1	1.1	1.1	1.1	1.1
Total error (%)		1.9	1.9	1.4	1.4	10.5	6.2
Thin target ($T\approx0.8$)							
Random error (%)	Current integration	0.2	0.2	0.2	0.2	0.2	0.2
	Particle loss	0.5	0.5	...	...	5	5
	Collimator background	0.2	0.2	0.2	0.2	50	5
	Target thickness	0.5	0.5	...	...	0.5	0.5
	Random rms error	0.8	0.8	0.3	0.3	50	7.1
Systematic error (%)	Electron energy	1	1	1	1	1	1
	Target purity	0.1	0.1	0.1	0.1	0.1	0.1
	Total systematic error	1.1	1.1	1.1	1.1	1.1	1.1
Total error (%)		1.9	1.9	1.4	1.4	51	8.2

diam targets from 0.5 to 20% of the backscattered charge. The uncertainty in this loss is estimated to be ±20%. Correction for change in geometry with target thickness was made to the backscattered charge and total charge.

4. *Target Thickness*

The uncertainty in average target thickness was less than 0.5%. An additional systematic error of 0.1% is estimated for target impurities and possible target misalignment.

The errors in typical runs for Al and U at 6.0 and 10.2 MeV for the transmission, absorption, and backscattering coefficients in thin and thick targets are given in Tables I and II, respectively.

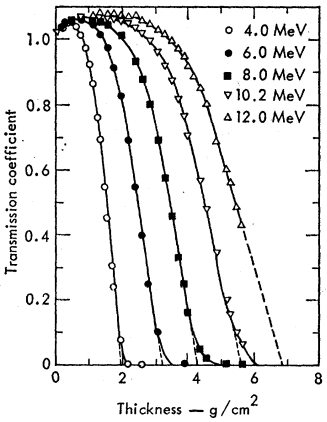

FIG. 2. Transmission coefficients as a function of C target thickness at 4.0-, 6.0-, 8.0-, 10.2-, and 12.0-MeV electron energies. Smooth curves connect experimental values.

III. EXPERIMENTAL RESULTS AND DISCUSSION

A. Transmission Coefficients

Transmission coefficients were calculated according to (1) after correcting for particle loss and background charge. They are plotted in Figs. 2–7. The Monte Carlo results of Berger and Seltzer[18] at 10.0 MeV are compared with experiment in Fig. 8.

1. *Extrapolated Range*

One characteristic of transmission curves for monoenergetic electrons incident on a planar target is the

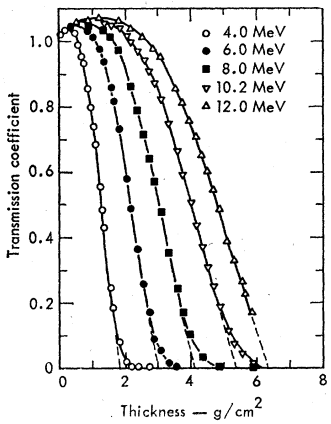

FIG. 3. Transmission coefficients as a function of Al target thickness at 4.0-, 6.0-, 8.0-, 10.2-, and 12.0-MeV electron energies. Smooth curves connect experimental values.

[18] M. J. Berger and S. M. Seltzer (private communication); calculation carried out with program ETRAN 15 described in M. J. Berger and S. M. Seltzer, National Aeronautics and Space Administration Report No. SP-169, 1968 (unpublished).

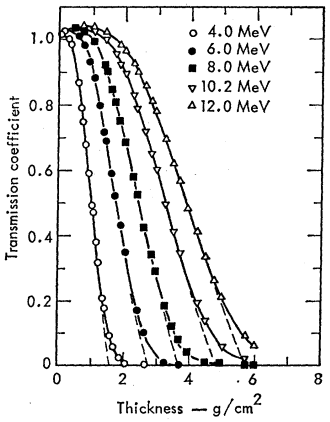

FIG. 4. Transmission coefficients as a function of Cu target thickness at 4.0-, 6.0-, 8.0-, 10.2-, and 12.0-MeV electron energies. Smooth curves connect experimental values.

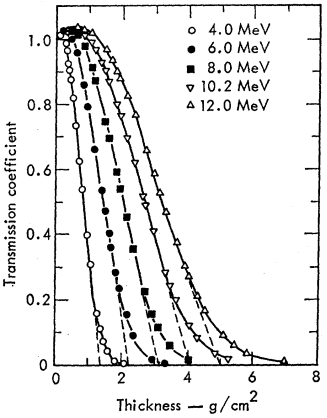

FIG. 5. Transmission coefficients as a function of Ag target thickness at 4.0-, 6.0-, 8.0-, 10.2-, and 12.0-MeV electron energies. Smooth curves connect experimental values.

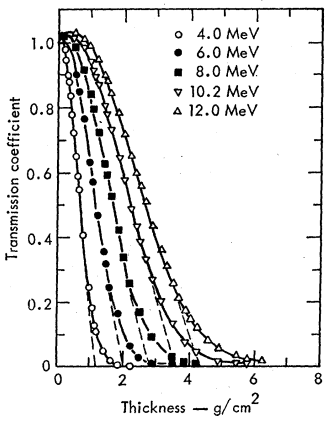

FIG. 6. Transmission coefficients as a function of Ta target thickness at 4.0-, 6.0-, 8.0-, 10.2-, and 12.0-MeV electron energies. Smooth curves connect experimental values.

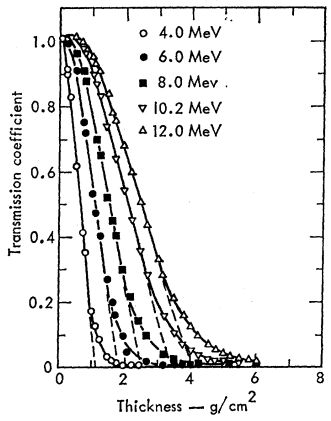

FIG. 7. Transmission coefficients as a function of U target thickness at 4.0-, 6.0-, 8.0-, 10.2-, and 12.0-MeV electron energies. Smooth curves connect experimental values.

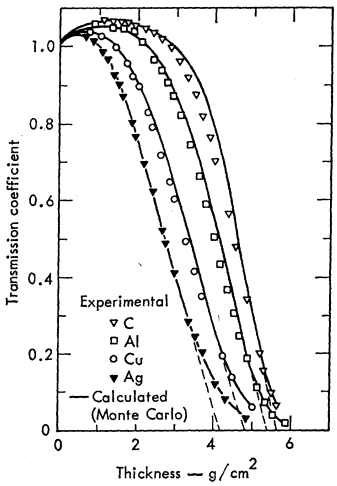

FIG. 8. Measured transmission coefficients at 10.2 MeV are compared with Monte Carlo results of Berger and Seltzer.

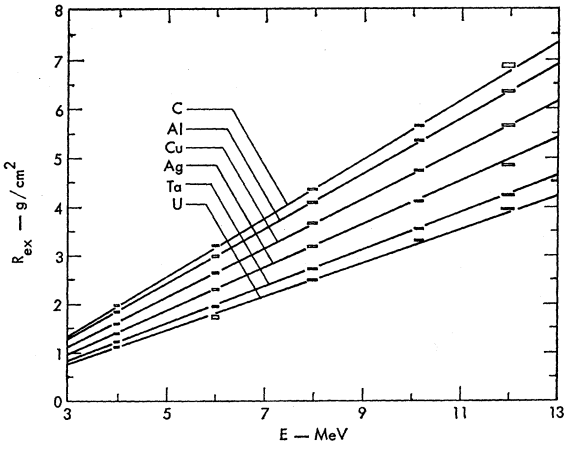

FIG. 9. Extrapolated range as a function of electron energy for C, Al, Cu, Ag, Ta, and U. The errors are reflected in the sizes of the points. The straight lines are given by R_{ex} (g/cm²) $=0.565[125/(Z+112)]E-0.423[175/(Z+162)]$, where E is in units of MeV.

straight-line portion, which, when extrapolated to zero transmission, gives the "extrapolated range" of the electron. The straight-line part of each of the curves shown in Figs. 2–7 was fit by the method of least squares for $0.2 \leq T \leq 0.8$. The $T=0$ intercept is plotted as a function of energy in Fig. 9. The errors in energy and in extrapolating to $T=0$ are indicated by the size of each point. The solid lines shown are given by the expression

$$R_{ex}\ (\mathrm{g/cm^2}) = 0.565\left(\frac{125}{Z+112}\right)E - 0.423\left(\frac{175}{Z+162}\right), \quad (4)$$

where E is in units of MeV.

While the slope and intercept of (4) are different from those given by Katz and Penfold[1] for Al, the extrapolated ranges given by (4) are very close to the values predicted by the Katz-Penfold formula.

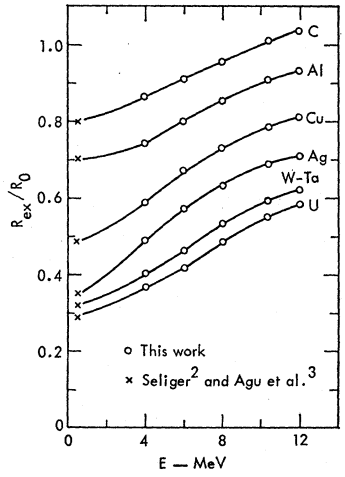

FIG. 10. Extrapolated range R_{ex} divided by the average path length R_0 as a function of electron energy.

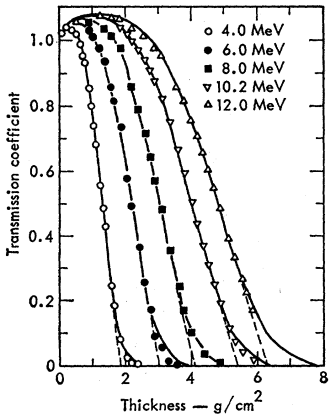

FIG. 11. Measured transmission coefficients (data points) in Al are compared with calculated coefficients (smooth curves) which are obtained from the sum of Eqs. (5) and (8).

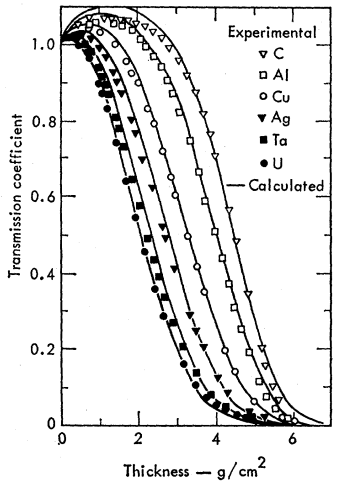

FIG. 12. Measured transmission coefficients at 10.2 MeV are compared with calculated coefficients.

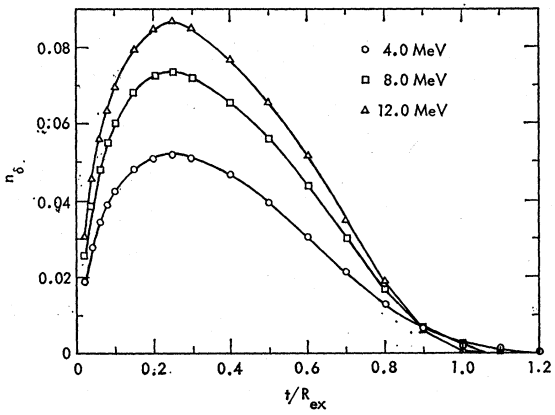

FIG. 13. Secondary electron contribution n_δ from Eq. (8) as a function of Al target thickness at 4.0, 8.0, and 12.0 MeV.

Berger and Seltzer[19] have computed the average electron path length assuming that the electron continuously loses energy in slowing down. Figure 10 shows the ratio of the extrapolated range according to (4) divided by the Berger-Seltzer average path length R_0. This experiment shows that R_{ex}/R_0 increases with increasing energy, and for the case of carbon at 10.2 and 12.0 MeV is ≥ 1. This is because of the statistical nature of the electron energy loss, and the fact that the multiple-scattering angular distribution peaks more forward with increasing electron energy.

2. *Empirical Transmission Equation*

Berger and Seltzer have demonstrated the power of Monte Carlo in calculating electron-transport phe-

[19] M. J. Berger and S. M. Seltzer, *Studies in Penetration of Charged Particles in Matter* [National Academy of Sciences–National Research Council (Publication No. 1133), Washington, D. C., 1964], p. 205.

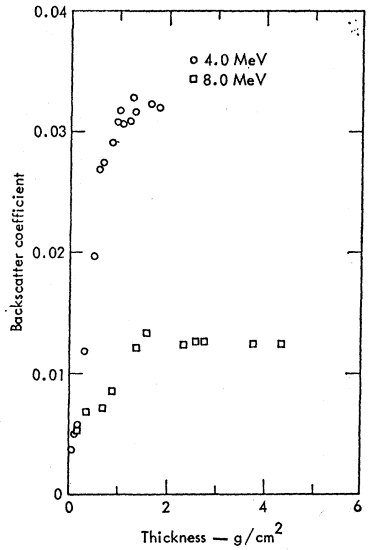

FIG. 14. Backscattering coefficients as a function of Al target thickness at 4.0 and 8.0 MeV.

nomena. It is useful, however, to have an empirical expression for rapid calculation of electron transmission.

Using data below 100 keV, Makhov[20] has formulated an empirical transmission equation in terms of the dimensionless variable t/R_0, where t is the target thickness and R_0 is the average path length of an electron having energy E. Mar[7] has formulated an empirical transmission equation for various elements,

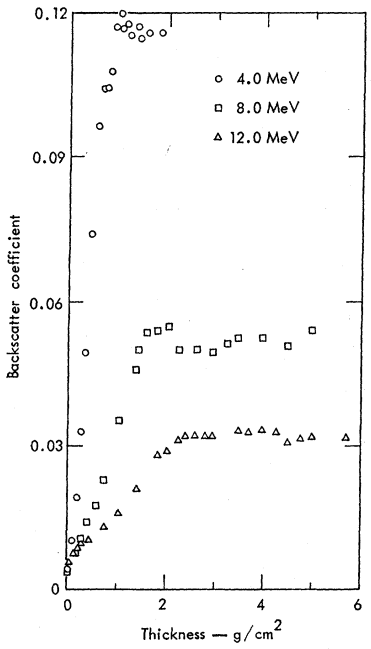

FIG. 15. Backscattering coefficients as a function of Cu target thickness at 4.0, 8.0, and 12.0 MeV.

[20] A. F. Makhov, Fiz. Tverd. Tela **2**, 2161 (1960) [English transl.: Soviet Phys.—Solid State **9**, 1934 (1961)].

using data reported by Marshall and Ward[21] and by Katz and Penfold[1] together with Monte Carlo results. Mar's expression gives the electron extrapolated range proportional to $E^{1.18}$, and while the transmission according to Mar agrees fairly well with results of this experiment at 4.0 MeV, the agreement is poor at higher energies. Better agreement can be achieved with a linear dependence of extrapolated range on energy. To achieve this dependence, we have assumed a transmission equation of the form

$$T=\exp[-\alpha(t/R_{ex})^{\beta}], \tag{5}$$

where α and β are functions of Z and E, which are determined by experiment. The slope of (5) at the point of inflection must extrapolate to R_{ex} when $T=0$. This requirement gives

$$\alpha=(1-1/\beta)^{1-\beta}. \tag{6}$$

Since $T>1$ for small t, this expression was fitted to the

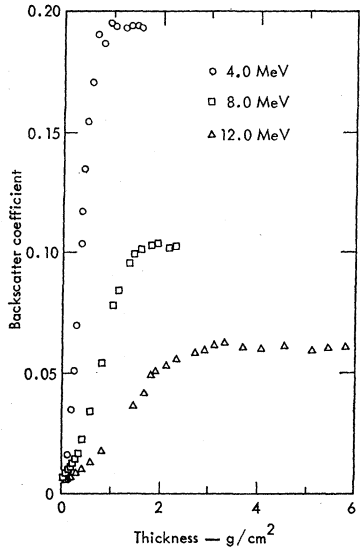

FIG. 16. Backscattering coefficients as a function of Ag target thickness at 4.0, 8.0, and 12.0 MeV.

experimental results for $T<0.5$, yielding

$$\beta=[387E/Z(1+7.5\times10^{-5}ZE^2)]^{0.25},\ E \text{ in MeV}. \tag{7}$$

That T is greater than 1, for small t, is a consequence of high-energy secondary electrons or δ rays escaping the target.

3. δ-Ray Production

Since all measurements were taken with a 500-V retarding bias, it is unlikely that very low-energy electrons originating from the target surface would influence measurement of the transmission, absorption, or backscattering coefficients. High-energy secondary

[21] J. S. Marshall and A. G. Ward, Can. J. Res. **15A**, 39 (1937).

electrons resulting both from hard electron-electron collisions (δ rays) and from bremsstrahlung produced in the target do contribute to the transmission. If the major fraction of secondary electrons were due to bremsstrahlung, then the maximum transmission would increase with Z. Since this is not the case, the additional electrons to give $T>1$ must primarily be δ rays having enough energy to escape the target. An expression for calculating γ-ray-induced secondary-electron escape[22] has been modified to calculate the number of δ rays escaping. The number of δ rays per incident electron escaping a target of thickness t can be expressed as

$$n_\delta=\frac{N_0Z}{A}\int_{\theta_{\min}}^{\pi/2}\int_0^t T(E_0,Z,x)\times\frac{d\sigma[E(x)]}{d\Omega}T\left(E(\theta),Z,\frac{t-x}{\cos\theta}\right)dx\,d\Omega, \quad (8)$$

where N_0 is Avogadro's number, $d\sigma[E(x)]/d\Omega$ is the relativistic Møller cross section[23] for an electron having energy $E(x)$, $T(E_0,Z,x)$ is the probability that an incident electron having initial energy E_0 will penetrate to depth x, and $T[E(\theta),Z,(t-x)/\cos\theta]$ is the probability that a secondary electron produced at x having energy $E(\theta)$ and direction θ will escape the target. In this expression, it is assumed that the δ ray travels to a target surface perpendicular to θ. Taking into account the average energy loss as the incident electron traverses the target, the integration is carried out from $\theta_{\min}$ to $\frac{1}{2}\pi$. $\theta_{\min}$ is the scattering angle at which half the primary electron energy is lost and is given by

$$\theta_{\min}=\cos^{-1}[(E+1.02)/(E+2.04)]^{1/2},\ E \text{ in MeV}. \quad (9)$$

When n_δ is added to T, given by (5)–(7), agreement to within $\pm 3\%$ of experiment is generally achieved, as seen in Figs. 11 and 12. Figure 13 shows n_δ from (8) for Al at $E=4.0$, 8.0, and 12.0 MeV.

B. Electron Backscattering

Backscattering coefficients were calculated according to (2) after correcting for particle loss and background charge. Backscattering coefficients as a function of target thickness for Al, Cu, Ag, and U are plotted for a few energies in Figs. 14–17.

Koral and Cohen[24] and Tabata[15] obtained good agreement for backscattering as a function of thickness with an empirical expression having the form

$$B(t)/B_s=1+a-e^{-b(2t/R_{ex})^n}, \quad (10)$$

where $B(t)$ is the backscattering coefficient for thickness t, B_s is the saturation backscattering coefficient, and a, b, and n are parameters independent of E (in the energy range 0.6–1.8 MeV and at 6.0 MeV) but dependent on Z. The results of this experiment indicate that $B(t)/B_s$ is more closely related to $t_{1/2}$ rather than R_{ex}, where $t_{1/2}$ is that thickness at which the transmission coefficient is 0.5. The data shown in Figs. 14–17 tend to confirm the result of both Tabata[15] and Cohen and Koral,[12] namely, that there is a nonzero intercept in the backscattering coefficient for very small target thickness. The experimental uncertainties were too large, however, to obtain accurate values of B for very thin targets. The

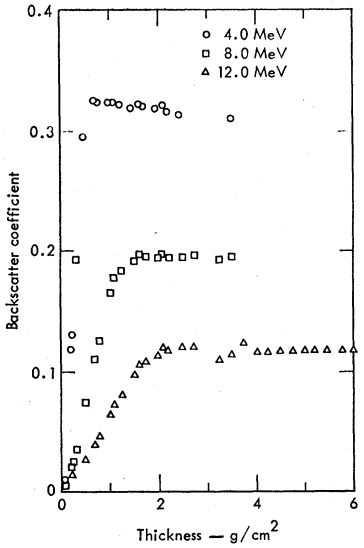

FIG. 17. Backscattering coefficients as a function of U target thickness at 4.0, 8.0, and 12.0 MeV.

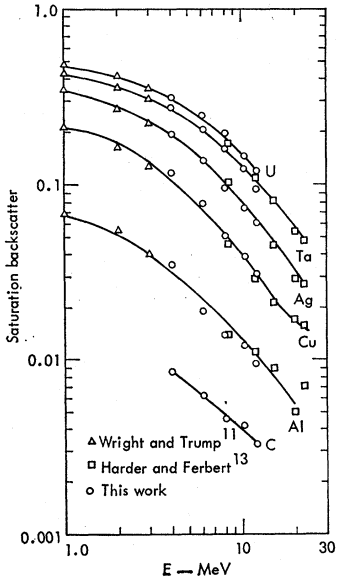

FIG. 18. Saturation backscattering as a function of electron energy for C, Al, Cu, Ag, Ta, and U.

[22] P. J. Ebert and A. F. Lauzon, IEEE Trans. Nucl. Sci. **NS-13**, 735 (1966).
[23] C. Møller, Ann. Physik, **14**, 531 (1932).
[24] K. F. Koral and A. J. Cohen, National Aeronautics and pace Administration Technical Note No. TND-2909, 1965 npublished).

TABLE III. Saturation backscattering coefficients B_s for C, Al, Cu, Ag, Ta, and U at 4.0, 6.0, 8.0, 10.2, and 12.0 MeV.

E (MeV)	Ref.	B_s C	Al	Cu	Ag	Ta	U
4.0	This work	0.009	0.035	0.117	0.195	0.276	0.317
	Tabata[a]	0.0070	0.032	0.102	0.179	0.274[b]	0.295
	Dressel[c]	0.0150	0.062	0.216	0.35	0.51	0.58
	Eq. (15)	0.012	0.049	0.117	0.183	0.269	0.326
6.0	This work	0.006	0.019	0.079	0.139	0.209	0.245
	Tabata[a]	0.005	0.018	0.068	0.129	0.206[b]	0.228
	Dressel[c,d]	0.010	0.035	0.140	0.24	0.43	0.45
	Eq. (15)	0.0	0.027	0.078	0.126	0.189	0.231
8.0	This work	0.005	0.014	0.051	0.095	0.160	0.195
	Tabata[a,d]	0.004	0.0142	0.049	0.097	0.169[b]	0.172
	Dressel[c,d]	0.0086	0.026	0.11	0.20	0.33	0.38
	Eq. (15)	...	0.015	0.056	0.095	0.146	0.180
10.2	This work	0.004	0.012	0.039	0.074	0.124	0.147
	Tabata[a]	0.0032	0.0097	0.0365	0.0735	0.127[b]	0.136
	Dressel[c,d]	0.009	0.024	0.092	0.18	0.28	0.33
	Eq. (15)		0.007	0.041	0.074	0.116	0.145
	Berger and Seltzer[e]	0.0055	0.013	0.041	0.081	0.145[f]	
12.0	This work	0.003	0.0096	0.031	0.061	0.095	0.120
	Tabata[a,d]	0.0031	0.0082	0.030	0.061	0.102[b]	0.112
	Dressel[c]	...	...	...	...	...	...
	Eq. (15)	...	0.002	0.032	0.061	0.099	0.124

[a] Reference 15. [b] Compared with Au. [c] Reference 14. [d] Interpolated. [e] Reference 18. [f] Calculated for Pb.

expression

$$B(t)/B_s=1-e^{-(2t/t_{1/2})^2} \tag{11}$$

was found to fit the experimental data except for small values of thickness. The experimentally determined values of $t_{1/2}$ are given by

$$t_{1/2}=\frac{1.2E^{1.21}}{(Z+13)^{0.5}}=\frac{R_{ex}}{\alpha}(\ln 2)^{1/\beta}, \quad E \text{ in MeV}. \tag{12}$$

Saturation backscattering coefficients are compared with those of other workers in Table III. The data listed in Table III are in excellent agreement with those reported by Tabata,[15] and in marked disagreement with those reported by Dressel.[14] Also listed in the table are Berger-Seltzer Monte Carlo results at 10 MeV. Again the agreement is excellent. Saturation backscattering coefficients are consistent with those reported by Wright and Trump[11] and by Harder and Ferbert,[13] as seen in Fig. 18. An expression valid in this energy range for $Z \geqq 29$ is

$$B_s=0.0343[(Z/E)^{0.75}-1], \quad E \text{ in MeV}. \tag{13}$$

ACKNOWLEDGMENTS

We wish to thank W. U. Miller, who performed the mechanical design and the construction of the apparatus. Thanks are also due to H. Catron, D. Lasher, D. Clark, and R. Der, who helped take data. The helpful suggestions of W. C. Dickinson are also gratefully acknowledged. Finally, we wish to thank the Linac Operators of EG & G, Inc., Santa Barbara, for their assistance during the entire experiment.